

Figure S1. Targeting claustrum neurons for *in vivo* recordings, related to Figure 1.

(A) Epifluorescence microscopy images showing the anterior-posterior extent of the expression of Channelrhodopsin-2-YFP (ChR2-YFP) in claustrum neurons in an example animal showing the lack of labeled neurons in insular cortex and striatum. **(B)** Summary graph showing the selection of optogenetically responsive neurons (blue quadrant, $n = 142$ of 1216 units from 9 mice). **(C)** Summary plot showing the waveform correlation of laser-evoked spikes versus non-laser-evoked spikes against the mean latency to first spike after laser activation ($n = 1216$ analyzed neurons recorded inside and outside the claustrum, cutoffs for being identified as optotagged: Correlation > 0.9 and Latency < 7 ms). **(D)** Summary plot showing the probability of laser activation evoking a spike versus the mean latency to first spike after laser activation ($n = 1216$ analyzed neurons recorded inside and outside the claustrum, cutoffs for being identified as optotagged: Reliability > 0.3 and Latency < 7 ms). **(E)** Example waveforms from an optotagged unit. Purple waveforms represent the mean laser-evoked action potentials; grey waveforms represent the mean non-laser-evoked action potentials. **(F)** Outlines of the claustrum in one example animal defined by the locations of optogenetically modulated units during each recording session. Tetrodes were lowered $75 \mu\text{m}$ dorsoventrally between each recording session (see Methods). **(G-J)** Confocal images of the claustrum of an experimental animal stained for parvalbumin (G, magenta). Retrogradely transfected S1-projecting claustrum neurons express ChR2-YFP (green, H) and tdTomato (I). **(K-N)** High magnification, single-plane confocal images showing that PV and tdTomato/YFP expression are non-overlapping. Scale bars: 1 mm (A), $100 \mu\text{m}$ (G-J), $10 \mu\text{m}$ (K-N).

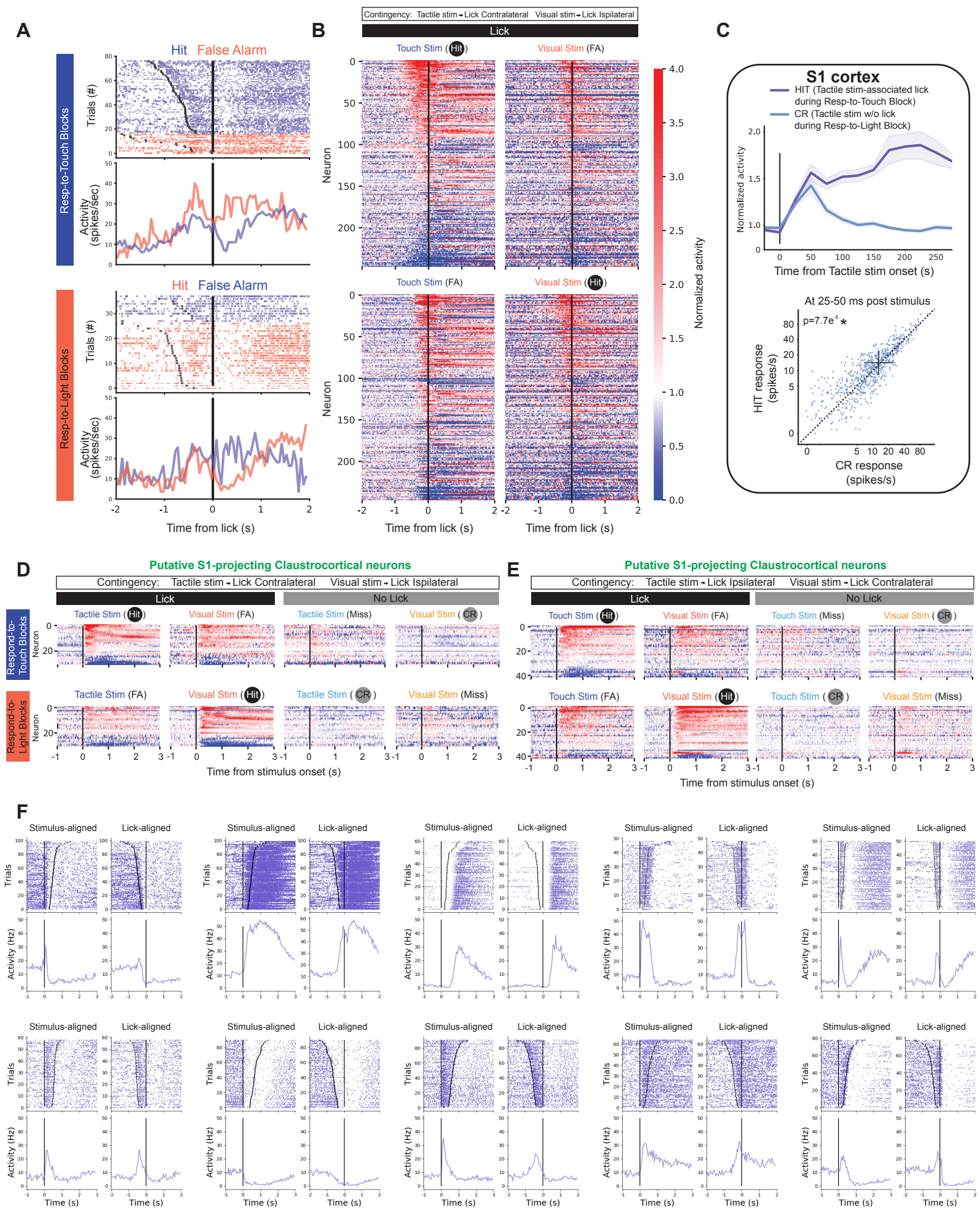


Figure S2. Claustrum and S1 neuron responses during a cross-modal sensory selection task, related to Figures 2 and 3.

(A) Raster plots and perlick time histograms for an example unit (same unit as in Figure 2A). Trials are sorted by block type (Top: Respond-to-Touch blocks, Bottom: Respond-to-Light blocks). For each block type, trials are color-coded by stimulus-response pairing (Touch blocks: Blue: Tactile Hits, Red: Visual False Alarms; Vision Blocks: Blue: Tactile False Alarms, Red: Visual Hits) and sorted by lick reaction time for Hit and False Alarm trials (Black dots: first lick). **(B)** Summary heatmaps showing mean activity aligned to the first lick, normalized to the -2 to -1 second baseline, for all claustrum neurons recorded in mice trained to respond to sensory stimuli with a contralateral lick during Respond-to-Touch blocks and an ipsilateral lick during Respond-to-Light blocks ($n = 247$ neurons, 6 mice, same neurons as Figure 2B). Neurons are in the same order as in Figure 2B. **(C)** Top plot: Normalized activity of neurons recorded in S1 during the task ($n = 754$ neurons from 4 mice, shaded areas represent the standard error). Light blue shows average response during Tactile stim-Correct Rejection trials in Respond-to-Light blocks and dark blue shows average response during Tactile-Hit trials in Respond-to-Touch blocks. Bottom plot: Scatter plot comparing the response of each S1 neuron during Tactile stim-Correct Rejection trials in Respond-to-Light blocks versus Tactile-Hit trials during Respond-to-Touch blocks at 25-50 ms following stimulus presentation (Tactile stim-Correct Rejection trials: 12.1 ± 0.53 spikes/s; Tactile-Hit trials: 13.3 ± 0.59 spikes/s, Wilcoxon signed-rank test, $p = 7.7e-5$). **(D,E)** Summary heatmaps showing mean stimulus-aligned activity, normalized to the unit's prestimulus baseline, for optotagged, putative S1-projecting claustrrocortical neurons recorded in mice trained to respond to sensory stimuli with a contralateral lick during Respond-to-Touch blocks and an ipsilateral lick during Respond-to-Light blocks (D, $n = 31$ units from 6 mice) and in mice trained to respond to sensory stimuli with an ipsilateral lick during Respond-to-Touch blocks and a contralateral lick during Respond-to-Light blocks (E, $n = 42$ units from 3 mice). **(F)** Example responses from ten individual claustrum neurons during Tactile Hit trials during Respond-to-Touch blocks shown aligned to the onset of the sensory stimulus (Stimulus-aligned, left panels) or the time of first detected lick (Lick-aligned, right panels). Blue dots show spikes; black dots show the first lick on Stimulus-aligned plots or the stimulus onset on Lick-aligned plots.

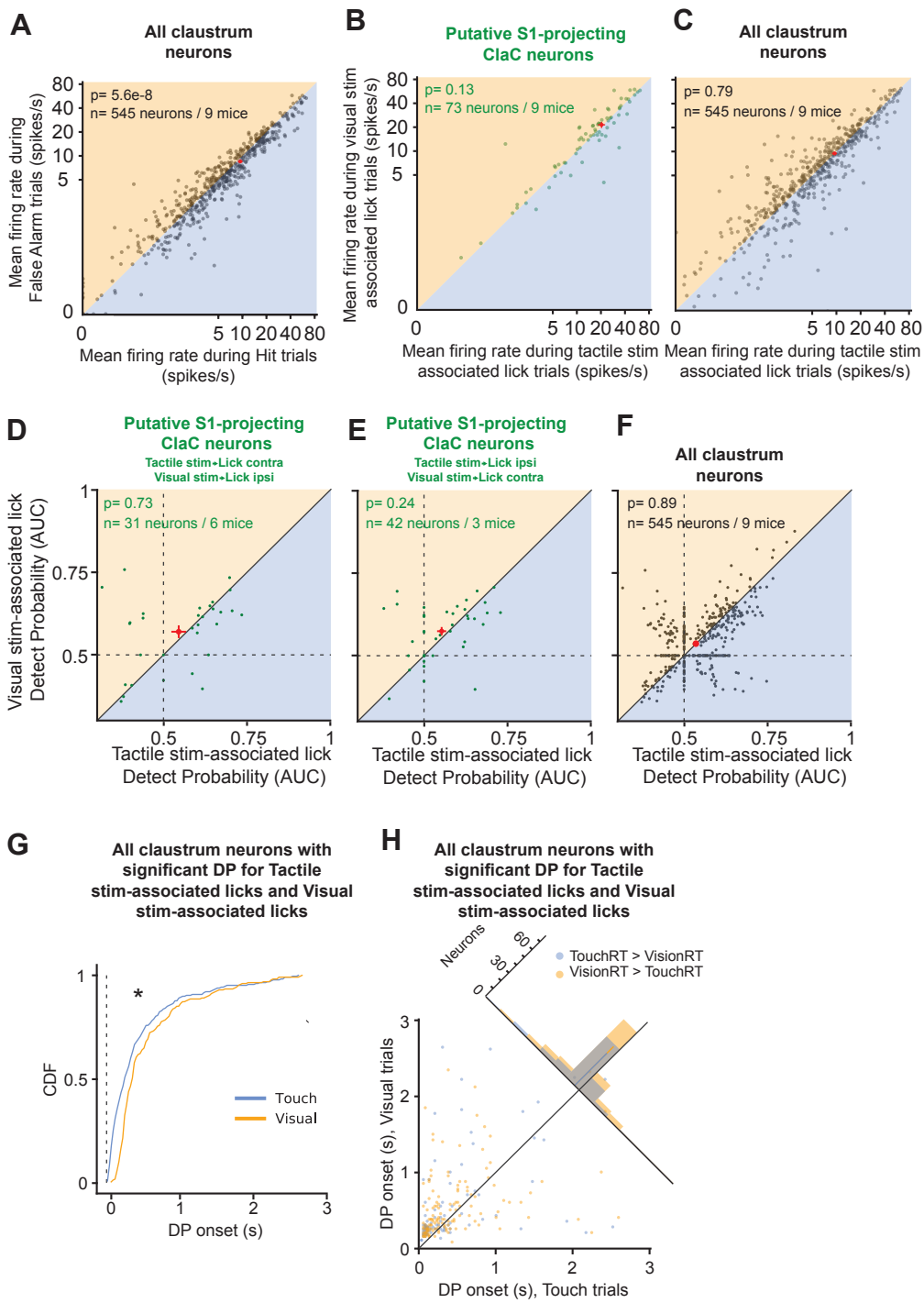
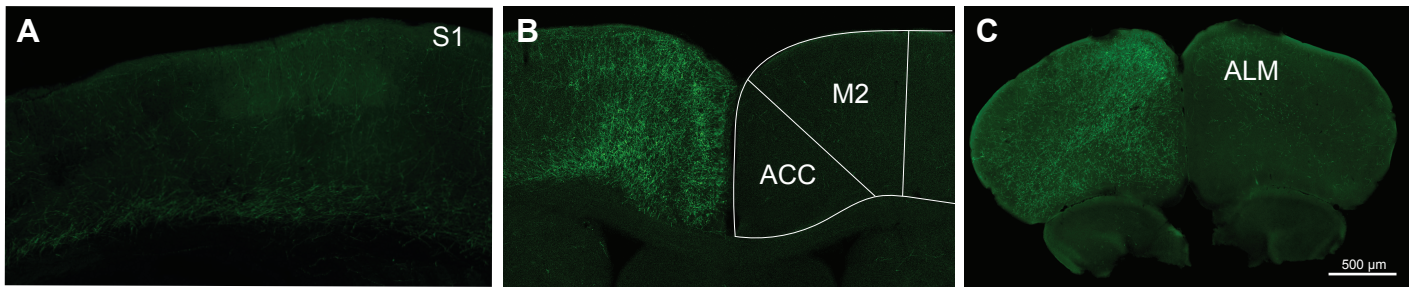


Figure S3. Comparison of the responses of claustrum neurons during visual and tactile Hit trials, related to Figure 3.

(A) Scatter plot of the mean firing rates of all recorded claustrum neurons for Hit trials versus False Alarm (FA) trials during the 1 second following stimulus onset (Hit trials: 9.37 ± 0.48 spikes/s, FA trials: 8.51 ± 0.42 spikes/s, $n = 545$ neurons, $N = 9$ mice, $p = 5.6e-8$, Wilcoxon signed-rank test, mean shown as red dot \pm SEM). **(B)** Scatter plot of the mean firing rates for Visual stim-associated lick trials versus Tactile stim-associated lick trials for optotagged, putative S1-projecting claustrum (ClaC) neurons during the 1 second following stimulus delivery (Tactile stim-associated lick trials: 19.6 ± 1.7 spikes/s, Visual stim-associated lick trials: 20.5 ± 1.8 spikes/s, $n = 73$ neurons from 9 mice, $p = 0.13$, Wilcoxon signed-rank test, mean shown as red dot \pm SEM). **(C)** Scatter plot of the mean firing rates for Visual stim-associated lick trials versus Tactile stim-associated lick trials for all recorded claustrum neurons during the 1 second following stimulus delivery (Tactile stim-associated lick trials: 9.4 ± 0.49 spikes/s; Visual stim-associated lick trials: 9.4 ± 0.48 spikes/s; $n = 545$ neurons; $p = 0.79$, Wilcoxon signed-rank test, mean shown as red dot \pm SEM). **(D)** Scatter plot showing the Detect Probability (DP) for visual stim-associated licks against tactile stim-associated licks for optotagged, putative S1-projecting ClaC neurons recorded in animals trained on Tactile stim-Contralateral lick ($n = 31$ neurons from 6 mice, mean score for 150 ms following DP onset, tactile stim-associated lick detect probability AUC = 0.55 ± 0.022 ; visual stim-associated lick detect probability AUC = 0.57 ± 0.019 ; Wilcoxon signed-rank test, $p = 0.73$, mean shown as red dot \pm SEM). **(E)** Scatter plot showing the DP for visual stim-associated licks against tactile stim-associated licks for optotagged, putative S1-projecting ClaC neurons recorded in animals trained on Tactile stim-Ipsilateral lick ($n = 42$ neurons from 3 mice, mean score for 150 ms following DP onset, touch-associated lick detect probability AUC = 0.55 ± 0.014 ; visual-associated lick detect probability AUC = 0.57 ± 0.013 ; $p = 0.24$, Wilcoxon signed-rank test, mean shown as red dot \pm SEM). **(F)** Scatter plot showing the DP for visual stim-associated licks against tactile stim-associated licks for all claustrum neurons recorded ($n = 545$ neurons from 9 mice, mean score for 150 ms following DP onset, tactile stim-associated lick detect probability AUC = 0.53 ± 0.0034 ; visual stim-associated lick detect probability AUC = 0.54 ± 0.0034 ; $p = 0.89$, Wilcoxon signed-rank test, mean shown as red dot \pm SEM). The 150 ms time window was chosen because it corresponds to a period that precedes the first lick based on the average reaction times of the mice. However, for each time window from 25 ms to 500 ms in 25 ms increments, the Bonferroni-corrected p value was not significant. Thus, varying the window used for this analysis does not affect the interpretation. The results were similar whether we tested only the subset of significantly modulated claustrum neurons (Touch: 0.56 ± 0.0080 , Vision: 0.57 ± 0.0076 , $n = 278$, $p = 0.78$, Wilcoxon signed-rank test), only the subset of claustrum neurons excited under both conditions (Touch: 0.63 ± 0.0045 , Vision: 0.62 ± 0.0049 , $n = 161$ neurons, $p = 0.12$, Wilcoxon signed-rank test), or only the subset of claustrum neurons inhibited under both conditions (Touch: 0.43 ± 0.0045 , Vision: 0.43 ± 0.0049 , $n = 50$ neurons, $p = 0.63$, Wilcoxon signed-rank Test). **(G)** Cumulative distribution frequency plot showing the distribution of DP onsets for tactile stim-associated licks and visual stim-associated licks, limited to neurons with significant DP for both trial types and onset post-stimulus delivery ($n = 228$ neurons from 9 mice; onset touch-associated lick AUC: 459 ± 35.6 ms; onset vision-associated lick AUC: 573 ± 34.6 ms; $p = 9.3e-9$, Wilcoxon signed-rank test). **(H)** Scatter plot comparing the DP onset for tactile stim-associated licks and visual stim-associated licks for neurons grouped by whether the median reaction time of the session was longer for touch

(blue, $n = 91$ neurons) or longer for visual trials (orange, $n = 137$ neurons). Corresponding histogram shows the distribution around the unity line ($p = 0.35$, Mann-Whitney U test on histogram counts).

Axonal projections from putative S1-projecting,
ChR2-YFP-expressing claustricortical neurons.



ALM innervation of claustrum

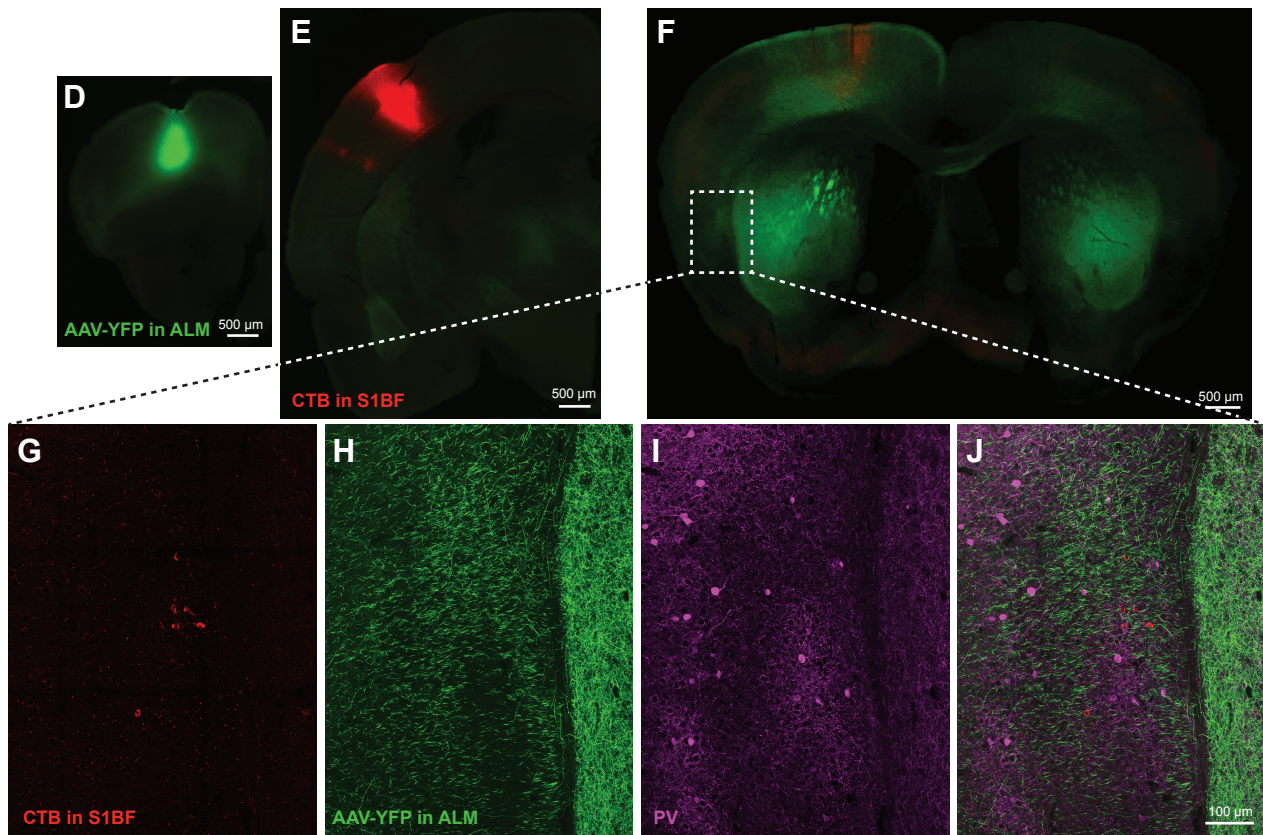


Figure S4. The claustrum and anterior lateral motor cortex (ALM) are reciprocally connected, related to Figure 4.

(A-C) Confocal images showing the axons of ChR2-YFP-expressing, S1-projecting claustrrocortical neurons labeled by our viral strategy. Neurons were labeled via their axonal projections in S1 (A) but most densely innervated frontal areas such as M2 (B) and the anterior lateral motor cortex (ALM; C). **(D,E)** Injection sites of an AAV-YFP viral vector into ALM (D, green) and of a retrograde tracer, Alexa-555 conjugated Cholera Toxin B (CTB), in the S1BF (E, red). **(F)** Low magnification image of the region shown at higher magnification in G-J. **(G-J)** Higher magnification images showing retrogradely labeled claustrrocortical (Clac) neurons projecting to S1BF (G, red), the innervation pattern of corticoclaustral axons projecting from ALM to the claustrum (H, green) and immunostained parvalbumin-positive (PV) neurons demarcating the claustrum core (I, magenta). These images are overlaid in J. Scale bars: 500 μm (A-F), 100 μm (G-J).

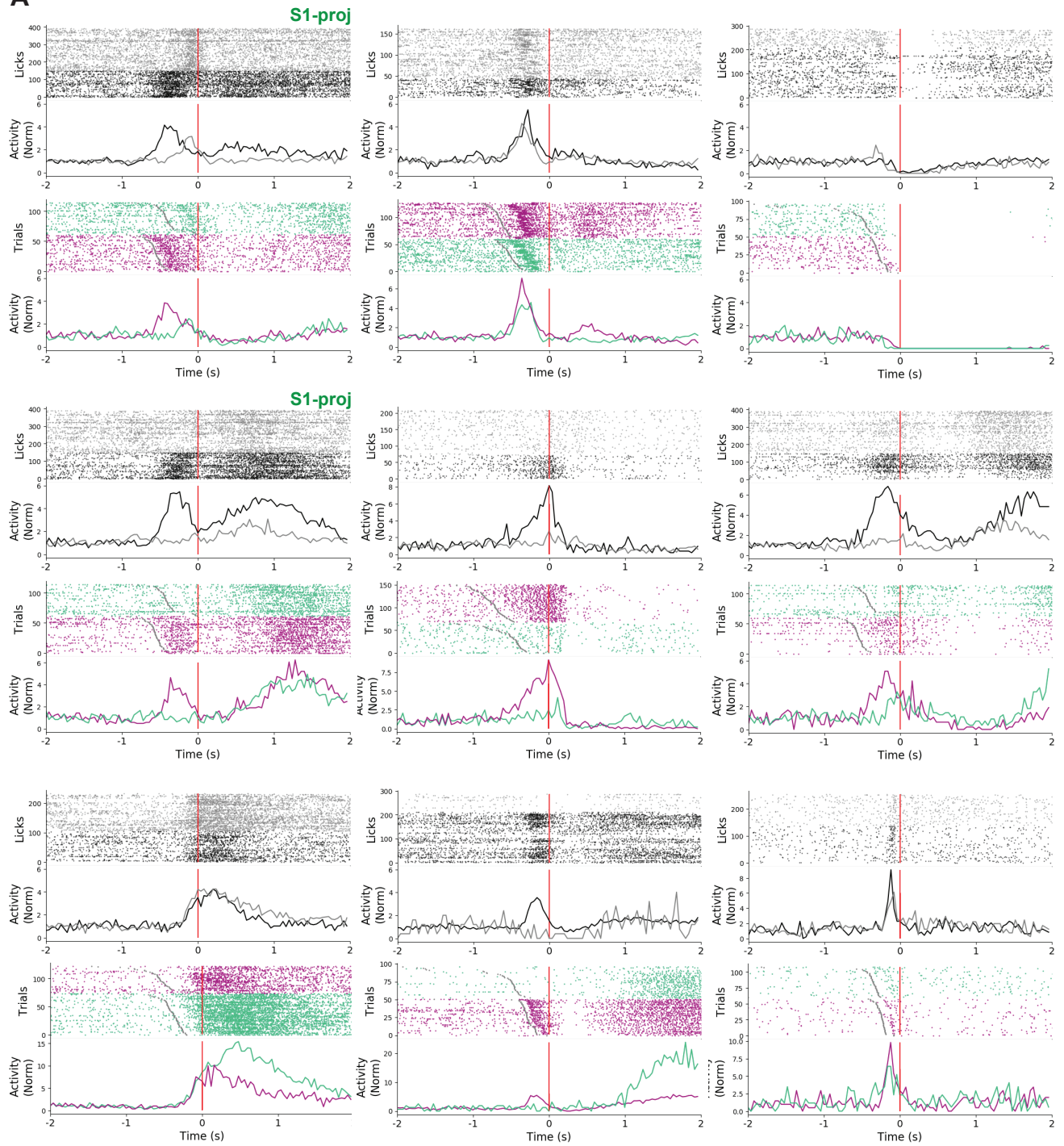
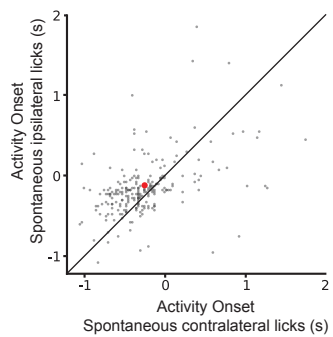
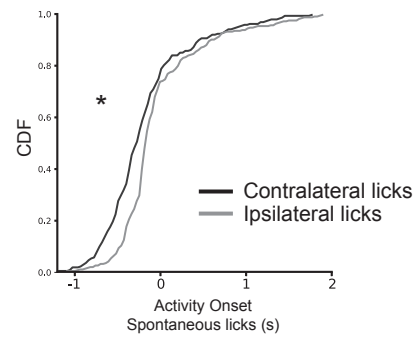
A**B****C**

Figure S5. Responses of claustrum neurons during spontaneous and task-evoked licks. Related to Figure 4.

(A) Raster plots and perlick time histograms for nine example claustrum neurons showing the correspondence between spontaneous lick activity and detection-associated lick activity (grey: spontaneous ipsilateral licks, black: spontaneous contralateral licks, green: detection-associated ipsilateral licks, purple: detection-associated contralateral licks). The two neurons marked S1-proj (top left, middle left) were optotagged, putative S1-projecting ClaC neurons.

(B) Summary scatter plot of the onset of spontaneous ipsilateral versus contralateral lick activity for claustrum neurons that significantly responded to both lick directions ($n = 232$ neurons). Red dot shows mean \pm SEM. **(C)** Cumulative distribution of the onset of activity for spontaneous contralateral licks (black) and for spontaneous ipsilateral licks (grey) for the neurons in (B) ($n = 232$ neurons; mean contralateral lick onset: -243.1 ± 29.6 ms; mean ipsilateral lick onset: -151.4 ± 23.5 ms, $p = 2.5e-6$, Wilcoxon signed-rank test).

Correlations during 1 second following stimulus onset

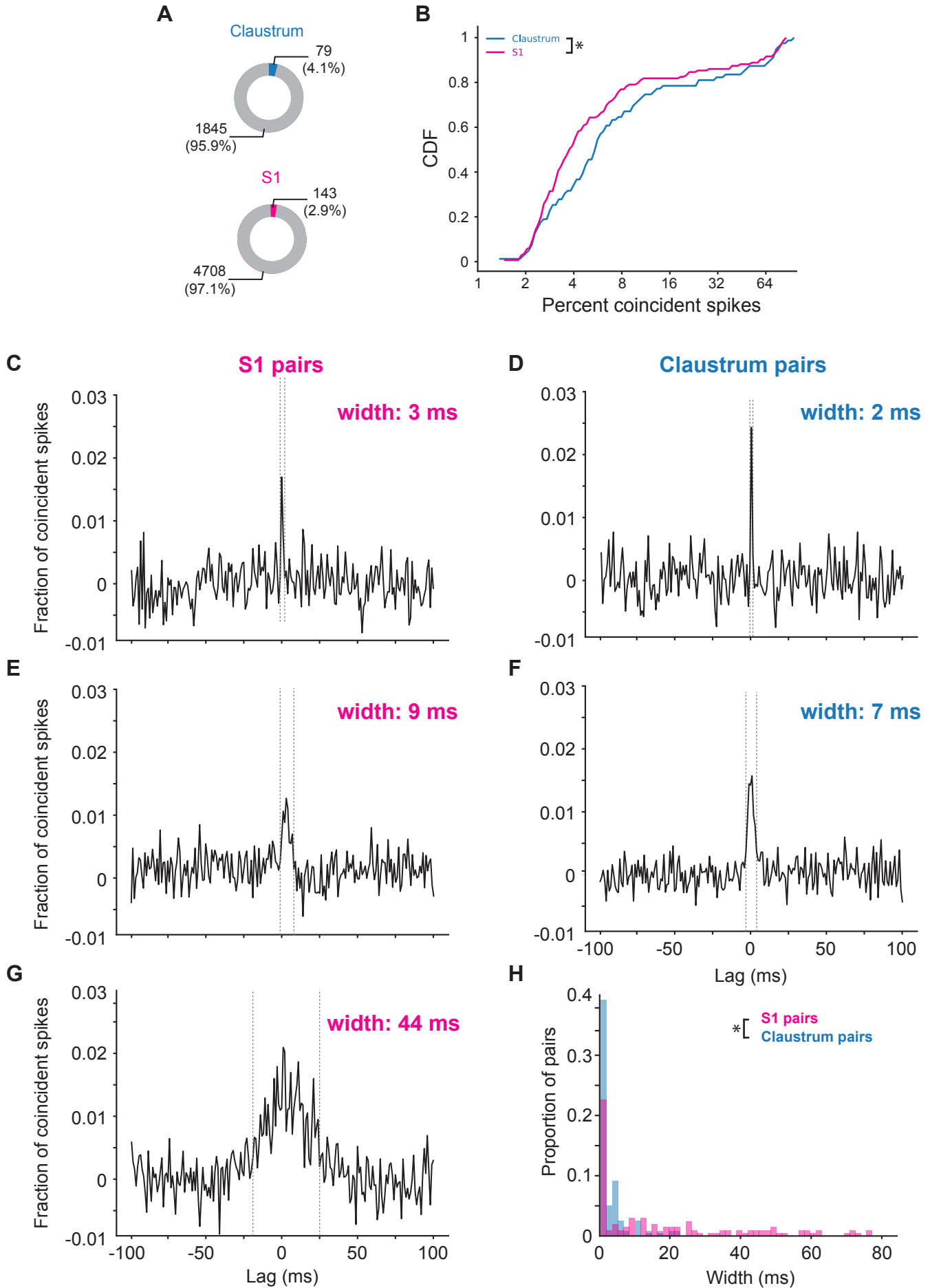


Figure S6. Claustrum neurons exhibit synchronous activity, related to Figure 5.

(A) Proportion of pairs of claustrum neurons (top) or S1 neurons (bottom) exhibiting significantly correlated activity during the 1 s following stimulus onset (blue, 79 of 1924 claustrum pairs; magenta, 143 of 4851 S1 pairs; $p = 0.0019$, Chi-Square test). The mean firing rates were higher in the 1 s following stimulus onset (Neurons in all pairs: S1: 10.04 ± 0.30 Hz, $n = 656$ S1 neurons; Claustrum: 7.58 ± 0.37 Hz, $n = 491$ claustrum neurons, $p = 1.13e-14$, Mann-Whitney U test; Neurons in correlated pairs: S1: 14.04 ± 0.92 Hz, $n = 141$ S1 neurons; Claustrum: 11.22 ± 0.97 Hz, $n = 112$ claustrum neurons, $p = 0.00512$, Mann-Whitney U test).

(B) Cumulative distribution of the percentage of coincident spikes for pairs of significantly correlated claustrum (blue, $n = 79$ pairs) and S1 neurons (magenta, $n = 143$ pairs) during the 1 s following stimulus onset (Claustrum pairs: $6.8 \pm 1.1\%$ mean coincident spikes, S1 pairs: mean $5.5 \pm 0.76\%$ coincident spikes; $p = 0.020$, Mann-Whitney U test). Note that the x-axis is \log_2 scaled. **(C-G)** Example unfiltered cross-correlograms for pairs of S1 neurons (C,E,G) and claustrum neurons (D,F) during the 1 s prior to stimulus onset, showing significantly correlated activity on different timescales. The dotted vertical lines show the width measurements for each crosscorrelogram. **(H)** Histogram showing the width of the crosscorrelograms for pairs of significantly correlated neurons during the 1 s prior to stimulus onset (Blue: Claustrum, $n = 75$ pairs, mean width: 3.5 ± 0.47 ms; Magenta: S1, $n = 129$ pairs, width: 21.6 ± 2.2 ; $p = 6.0e-8$, Mann-Whitney U test).

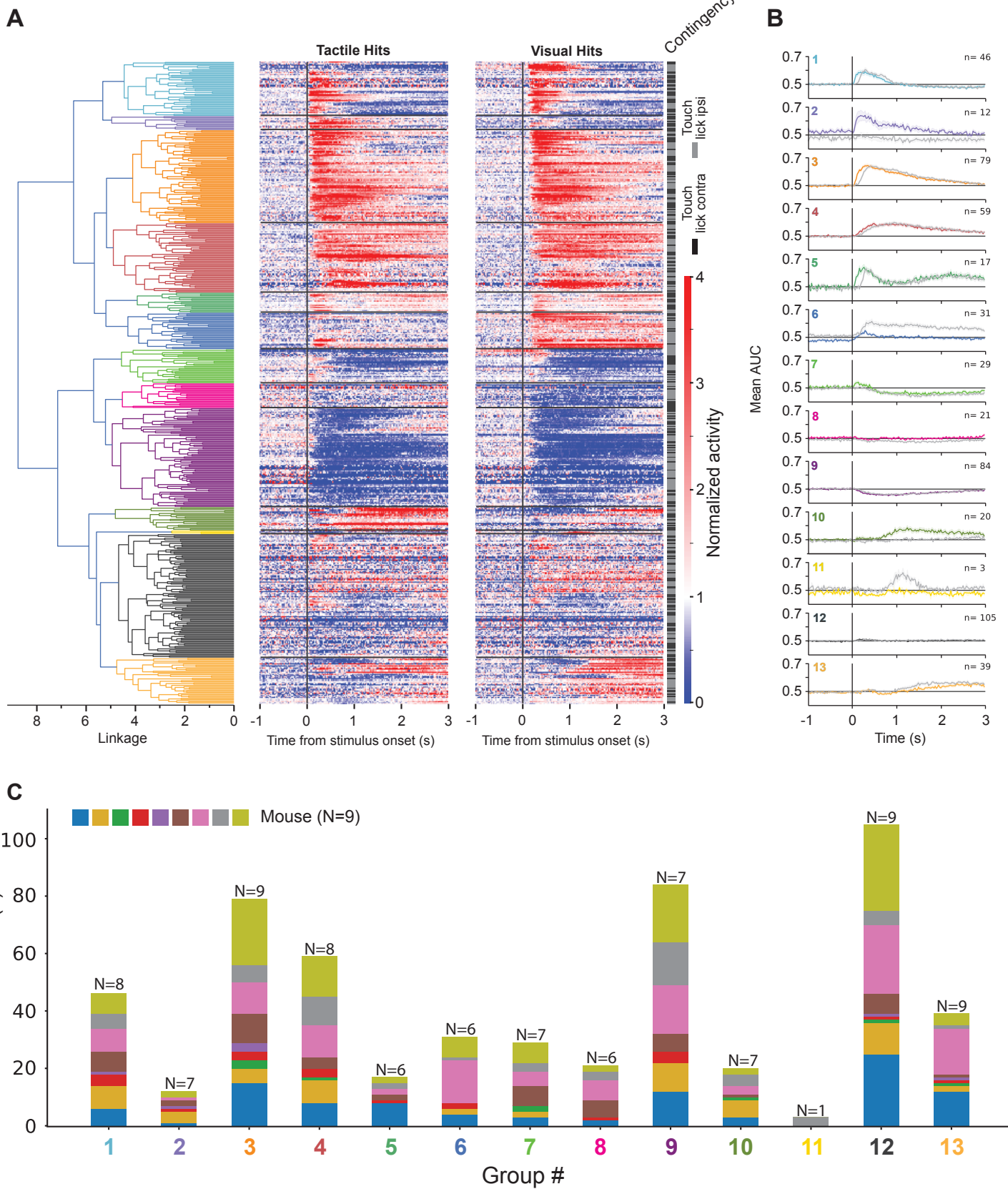


Figure S7. : Claustrum neurons exhibit diverse response profiles during the behavioral task, related to Figure 6.

(A) Hierarchical clustering of all recorded claustrum neurons based on their mean response during Hit trials. Heatmaps show the baseline-normalized, mean activity of each neuron to tactile stim-associated Hit trials (left panel) and visual stim-associated Hit trials (right panel) aligned to the stimulus onset. Dendrogram shows clustering results. The contingency column (black/grey) indicates whether a neuron was recorded from an animal trained to perform Touch-Contralateral/Vision-Ipsilateral (Black) or Touch-Ipsilateral/Vision-Contralateral (Grey) trials (n = 545 neurons from 9 mice). **(B)** Bar graph showing the number of neurons within each group and the animals from which the neurons were recorded. Above each bar is the total number of mice contributing to that group. Neurons from 6 or more mice contributed to each group, except for Group 11 composed of just 3 neurons. All groups but Group 11 also included neurons recorded under both task contingencies.